

Nighttime Chemistry and Morning Isoprene Can Drive Urban Ozone Downwind of a Major Deciduous Forest

Dylan B. Millet,^{*,†} Munkhbayar Baasandorj,^{†,‡} Lu Hu,^{†,§} Dhruv Mitroo,^{||} Jay Turner,^{||} and Brent J. Williams^{||}

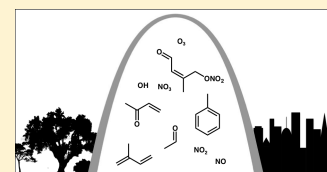
[†]University of Minnesota, St. Paul, Minnesota 55108, United States

^{||}Washington University in St. Louis, St. Louis, Missouri 63130, United States

S Supporting Information

ABSTRACT: Isoprene is the predominant non-methane volatile organic compound emitted to the atmosphere and shapes tropospheric composition and biogeochemistry through its effects on ozone, other oxidants, aerosols, and the nitrogen cycle. Isoprene is emitted naturally by vegetation during daytime, when its photo-oxidation is rapid, and in the presence of nitrogen oxides (NO_x) produces ozone and degrades air quality in polluted regions. Here, we show for a city downwind of an isoprene-emitting forest (St. Louis, MO) that isoprene actually peaks at night; ambient levels then endure, owing to low nighttime OH radical concentrations.

Nocturnal chemistry controls the fate of that isoprene and the likelihood of a high-ozone episode the following day. When nitrate (NO₃) radicals are suppressed, high isoprene persists through the night, providing photochemical fuel upon daybreak and leading to a dramatic late-morning ozone peak. On nights with significant NO₃, isoprene is removed before dawn; days with low morning isoprene then have lower ozone with a more typical afternoon peak. This biogenic–anthropogenic coupling expands the daily high-ozone window and likely has an opposite O₃–NO_x response to what would otherwise be expected, with implications for exposure and air-quality management in cities that, like St. Louis, are downwind of major isoprene-emitting forests.



1. INTRODUCTION

Approximately 1 Pg (10¹⁵ g) of non-methane volatile organic compounds (VOCs) is emitted to the atmosphere by land ecosystems each year, some 8× greater than the estimated anthropogenic source.^{1,2} Of these, isoprene (2-methyl-1,3-butadiene, C₅H₈) is predominant, accounting for half of the total known flux. Emitted mainly by deciduous trees and shrubs, isoprene quickly reacts by addition with the hydroxyl radical ($\tau \sim 1$ h at [OH] = 2.5×10^6 molecules cm⁻³; ref 3), producing hydroperoxy radicals that can oxidize NO to NO₂ and hence drive ozone (O₃) production.⁴ Because fuel combustion is the main source of atmospheric NO_x (NO + NO₂),^{5,6} this represents a major biogenic–anthropogenic interaction that for some time has been known to have important consequences for ozone air quality.^{7,8} Such biogenic–anthropogenic interactions involving isoprene have since been found to modulate aerosol formation^{9–12} as well as the transport and fate of atmospheric nitrogen.^{13–15}

Isoprene production is tied to photosynthesis and is strongly light- and temperature-dependent;¹⁶ as a result, emissions follow a pronounced diurnal cycle, peaking in the middle of the day and falling to zero at night.^{2,17} This diurnal cycle parallels that of photolytic OH production, and most isoprene molecules are thus oxidized during the day by OH. However, isoprene that is emitted close to dusk, when OH concentrations are dropping, can persist into the nighttime hours.^{18,19} Then, oxidation by ozone can continue but is slow ($\tau = 30$ h at [O₃] = 30 ppb; ref 3). Nitrate (NO₃) radicals, on the other hand, which are generated from the combination of NO₂ with O₃ and rapidly photolyzed during the day, can be abundant at night

and react rapidly with isoprene ($\tau = 20$ min at [NO₃] = 50 ppt; ref 3). The reaction proceeds by addition of NO₃ to one of isoprene's two double bonds and leads to a variety of multifunctional nitrates.²⁰ This chemistry is important because it can lead to aerosol (mainly via second- and higher generation products²¹), contributing to particulate pollution, and because it can represent a substantial sink or reservoir of NO_x.^{19,22} Here, we show for the first time that, for cities downwind of isoprene-emitting forests, such nighttime isoprene chemistry can have a critical impact on ozone air quality and photochemistry the following day.

2. METHODS

2.1. Field Measurements. We measured isoprene, its oxidation products methyl vinyl ketone (MVK) and methacrolein (MACR), and an ensemble of other trace gas, aerosol, and meteorological parameters during the St. Louis Air Quality Regional Study (SLAQRS). SLAQRS took place during August–September 2013 and was conducted at the St. Louis–Midwest Supersite core monitoring station located in East St. Louis, IL (38.6122 N, 90.16028 W, 184 m elevation). A detailed description of the site is given elsewhere.^{23,24} Isoprene (m/z 69), the sum of MVK + MACR (m/z 71), and a suite of other VOCs were measured with the University of Minnesota high-sensitivity quadrupole proton-transfer-reaction mass spec-

Received: December 30, 2015

Revised: March 20, 2016

Accepted: March 24, 2016

Published: March 24, 2016

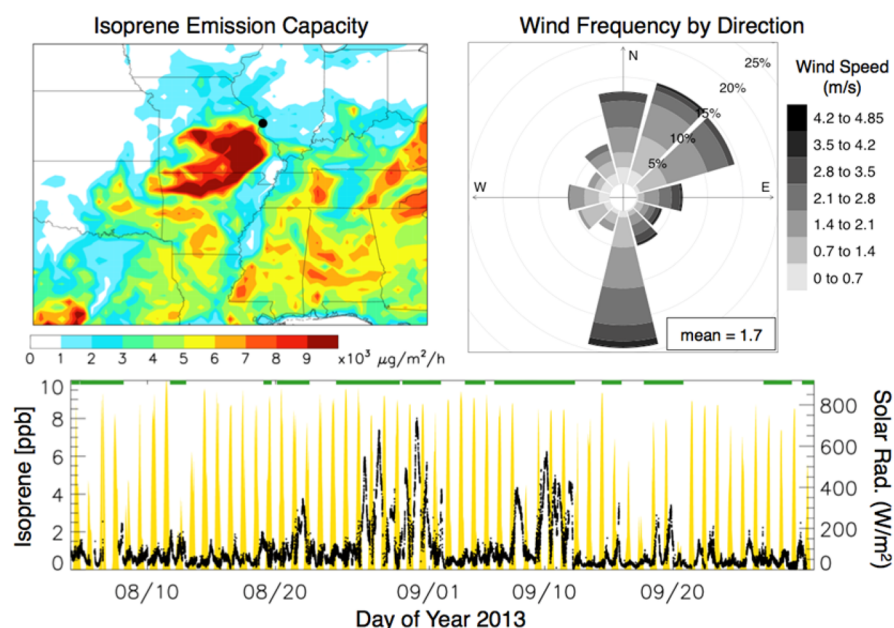


Figure 1. Isoprene measurements in St. Louis: (top left) isoprene emissions over the U.S. southeast estimated under standard conditions² with the black circle indicating the study location, (top right) frequency of observed wind direction and speed during the study, and (bottom) measured isoprene (black) and solar radiation (yellow). Green markings indicate periods with southerly winds (170–270°, >0.5 m/s).

trometer (PTR-MS, Ionicon Analytik GmbH) as described in earlier papers.^{25–27} Briefly, ambient air was drawn from the top of the trailer (5 m above ground) with a sampling flow of 10 standard liters per minute (slm) through 6 m of heated $1/2$ in. outer diameter perfluoroalkoxy (PFA) tubing. Of this, 1 slm was subsampled by the PTR-MS inlet system. The PTR-MS drift tube pressure and voltage were maintained at 2.3 mbar and 600 V ($E/N = 126$ Td), with the water flow at 6.5 standard cubic centimeters per minute (sccm); dwell times were 5–10 s for the various compounds measured. The abundance of H_3O^+ ions was $(1.2\text{--}2) \times 10^9$ counts per second (cps), with interference from O_2^+ amounting to less than 1% of the H_3O^+ signal. Zero air for instrument blanks was generated by passing ambient air over a heated Pt catalyst (450 °C) to maintain ambient humidity. Calibration was performed via dynamic dilution of multicomponent compressed gas standards (Apel-Riemer Environmental, Inc.) into a zero air stream generated in the same way, with these standards recertified in our laboratory prior to deployment using the custom-built permeation-based calibration apparatus described by Baasandorj et al.²⁷ As discussed in the [Supporting Information](#), we do not expect any measurement interferences for isoprene or MVK + MACR to impact the analyses shown here.

NO and NO_2 were measured during SLAQRS by chemiluminescence (42i-TL, Thermo Scientific, Inc.), and O_3 was quantified by ultraviolet (UV) absorption at 254 nm (49i, Thermo Scientific, Inc.). Both instruments were calibrated and drift-corrected regularly throughout the study (146i, Thermo Scientific, Inc.).

2.2. Dynamically Simple Model of Atmospheric Chemical Complexity (DSMACC). We use the DSMACC chemical box model developed by Emmerson and Evans²⁸ to interpret the SLAQRS observations. DSMACC is a zero-dimensional tropospheric chemistry box model^{28–31} employing the Kinetic PreProcessor (KPP)³² and the Tropospheric Ultraviolet and Visible (TUV) photolysis scheme.³³ The model can be used for both free-running and constrained

simulations and is designed for flexibility in accommodating different chemical mechanisms. The mechanism employed here is based on v9-02 of the GEOS-Chem chemical transport model, with isoprene oxidation as described by Mao et al.¹⁵ Model runs are performed for the SLAQRS site location and initialized at 9 pm local standard time on July 31 (298 K, 987.714 hPa, and $[H_2O] = 2$ mol %) with 8 ppb of isoprene, 2 ppb of MVK + MACR (1 ppb each), 200 ppb of CO, 1.82 ppm of CH_4 , 30 ppb of O_3 , and 10 ppb of NO_2 . We also include 2 ppb of PRPE (lumped species representing $\geq C_3$ alkenes) as a surrogate for other reactive VOCs. This is necessarily an approximation, because a full suite of VOCs was not measured during the study. Halving or doubling this assumption changes the magnitude of the model O_x enhancements discussed later but does not alter their timing or general features. NO is set to either 0.5 or 4 ppb, with mixing ratios then constrained to the initial value throughout the model run as a proxy for ongoing emissions into the urban atmosphere. Additional sensitivity analyses shown in [Figure S1](#) of the Supporting Information (and discussed later) include (i) a model run with no NO_3 + VOC reactions and (ii) a run in which reaction of NO_3 with isoprene is assumed to be a terminal sink for both species (e.g., the products then undergo deposition, aerosol uptake, or wet scavenging).

3. RESULTS AND DISCUSSION

[Figure 1](#) shows that St. Louis lies near (~ 35 km) the oak forests of the Ozark Plateau, a major isoprene source region with a growing season per area flux comparable to the tropical forests of Amazonia and Africa.^{34–36} In general, winds during the SLAQRS study were either northerly, bringing low-isoprene air from the predominantly agricultural landscapes of northern Missouri, southern Iowa, and southwestern Illinois, or from the south to southwest, bringing biogenically impacted air from the Ozarks. The bottom panel of [Figure 1](#) shows the consequence of these wind shifts: alternating regimes of low and extremely high isoprene. Conversely, anthropogenically emitted VOCs

show no such transitions and were elevated throughout the study.³⁷

A surprising aspect of the isoprene measurements shown in Figure 1 is that the peak concentrations (up to 8 ppb) occur at night. Such values would be unusually high even in many daytime forested environments (e.g., refs 38 and 39). However, they are consistent with earlier measurements in the upwind Ozark forest,³⁴ showing peak isoprene levels during late afternoon and early evening in the newly formed nocturnal boundary layer. Average surface concentrations in the upwind forest during that earlier study exceeded 25 ppb between 17:00 and 18:00 CST and were still extremely high (averaging ~13 ppb) between 20:00 and 21:00 CST.

During the southerly episodes observed during SLAQRS, midday isoprene levels (when emissions are highest) are comparatively low in the city. We attribute this to OH-driven photo-oxidation during daytime transport from the Ozarks: given a 2 m/s wind speed and OH of 2.5×10^6 molecules cm^{-3} , isoprene would undergo >4 *e*-foldings during a 4–5 h transit between the forest edge and the urban core. On the other hand, we see that a substantial amount of isoprene emitted during late afternoon survives past sunset and is transported to the city via southerly winds. The result is heavily isoprene-laden air entering the urban airshed at night.

The impact of that isoprene then depends upon the nocturnal chemical environment, as illustrated in Figure 2 for four example nights during the campaign. The figure shows that on Aug 3–4 and Aug 11–12 there occurred a strong decrease in the ambient isoprene concentrations following a peak in the early nighttime hours. We can explore the cause of the decline in each case using simultaneous measurements of MVK + MACR, which are produced in high yield from the oxidation of

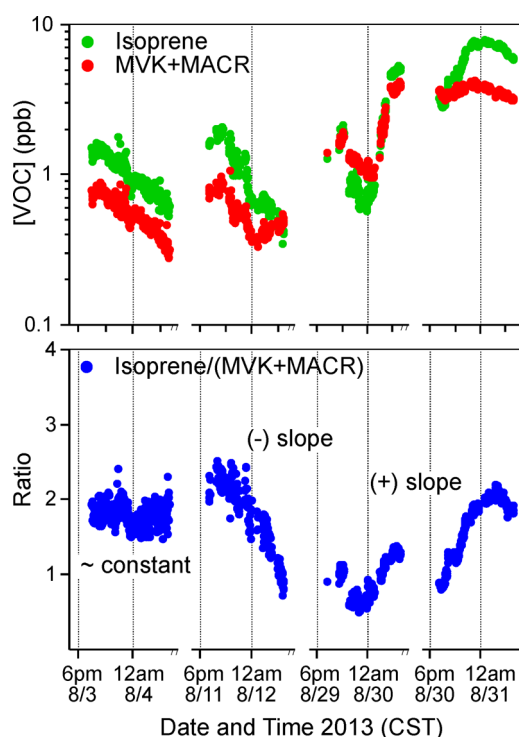


Figure 2. Nocturnal changes in isoprene and its oxidation products. Plotted are measurements of isoprene, the sum of its oxidation products MVK + MACR, and isoprene/(MVK + MACR) on four example nights during the campaign.

isoprene by OH or O_3 (and in very low yield from the oxidation of isoprene by NO_3).^{40–42} Because MVK and MACR are themselves much less reactive than isoprene toward these same oxidants,³ the isoprene/(MVK + MACR) ratio can be used as a proxy for the degree of oxidative aging since isoprene was emitted (with higher ratios indicating less chemical aging).^{43–45} The pronounced nighttime decrease in isoprene/(MVK + MACR) on Aug 11–12 thus implies chemical removal of isoprene during this time. On the other hand, the relatively constant isoprene/(MVK + MACR) ratios on Aug 3–4 indicate that the isoprene decline on this night was driven by atmospheric mixing and transport rather than chemistry. For the nights of Aug 29–30 and Aug 30–31, the isoprene/(MVK + MACR) ratio shows that, again, there was little or no oxidative chemistry occurring, and on both of these occasions isoprene concentrations exceeding 5 ppb were still present the following morning.

This night-to-night variability in isoprene oxidation and hence in the amount of isoprene still present at daybreak is driven by the abundance of NO_3 radicals. Figure 3 provides a more detailed look at this for two distinct nights with elevated isoprene concentrations. On the night of Aug 26–27, isoprene levels peaked at nearly 6 ppb before declining after midnight to approximately 2.5 ppb by 4:00 am. On the basis of concurrent measurements at the site, we can derive the rate of decline that would be expected due to isoprene's reaction with NO_3 and with O_3 (see the Supporting Information). Results are shown as red (reaction with O_3) and purple (reaction with NO_3 and with O_3) solid lines in Figure 3. We then attribute any remaining change to atmospheric mixing and transport effects and apply an exponential fit of the residuals to derive an effective dilution rate coefficient. The overall calculated trajectory due to O_3 chemistry, NO_3 chemistry, and mixing/transport is shown as the green line in Figure 3. We see in this case that the overall isoprene decline of 3.5 ppb over 4 h observed on this night can be attributed to approximately equal contributions from chemical oxidation and dilution, with NO_3 providing the majority of the oxidizing power.

Measurements of MVK + MACR over this same time period then provide a quantitative and independent test of the above attribution. Applying the chemical loss rates for MVK + MACR due to NO_3 and O_3 as above, while accounting for MVK + MACR production from the isoprene + O_3 and isoprene + NO_3 reactions and employing the same dilution frequency derived for isoprene, results in the solid gray line in Figure 3. The observed change in MVK + MACR thus corroborates the inferred isoprene sink estimates.

The night of Aug 30–31 brought a very different situation. Again, isoprene peaked around midnight (at 8 ppb), but in this case, the estimated NO_3 abundance was much lower. As a result, chemical loss of isoprene was minimal and 6 ppb of isoprene was still present at 4:00 am. As we show later, this has a large impact on ozone air quality during the ensuing day. Again, the MVK + MACR observations provide independent support for the above attribution (Figure 3).

What causes these differences in NO_3 chemistry between nights? Figure 3 shows that, for the time periods investigated above, NO was higher and O_3 was lower on Aug 30–31 (median 0:00–04:00 values of 1.4 and 6.5 ppb, respectively) than was the case on Aug 26–27 (0.5 and 11.1 ppb). High NO titrates O_3 , thus slowing NO_3 production via $\text{NO}_2 + \text{O}_3$, while also providing a direct NO_3 sink via $\text{NO}_3 + \text{NO}$. On the night of Aug 30–31, when we see negligible chemical loss of

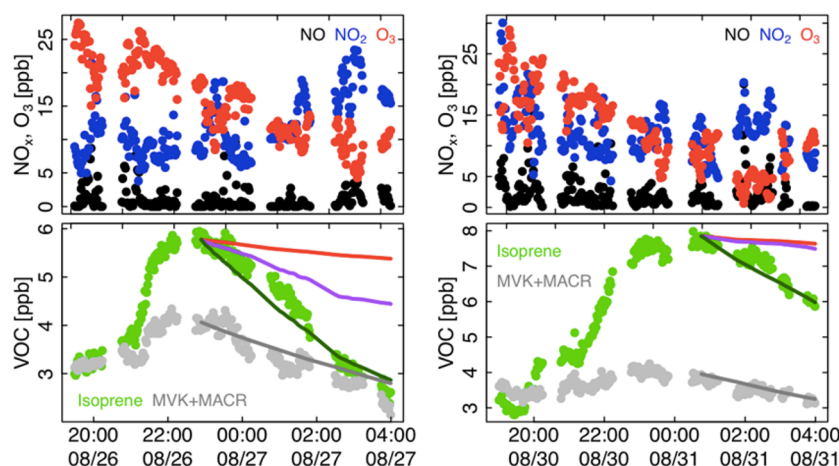


Figure 3. Nighttime isoprene removal. Shown are measurements of NO_x , O_3 , isoprene, and MVK + MACR on two nights with elevated isoprene. Solid lines show the calculated isoprene decay due to O_3 (red), $\text{O}_3 + \text{NO}_3$ (purple), and $\text{O}_3 + \text{NO}_3 + \text{mixing}$ (green), as described in the text. Gray lines show the resulting predictions for MVK + MACR. Time stamps indicate local standard time (CST).

isoprene, the mean NO_3 lifetime due to reaction with NO, $\tau_{\text{NO}_3(\text{NO})}$, is only 2 s. On the night of Aug 26–27, this lifetime, while still short (mean of 18 s), is nonetheless long enough that isoprene itself is a more important NO_3 sink (mean $\tau_{\text{NO}_3(\text{isoprene})} = 14$ s). When combined with $\sim 2\times$ more rapid NO_3 production, the estimated steady-state NO_3 abundance is some $5\times$ higher on this occasion, and we therefore see significant chemical removal of isoprene by night's end.

We carried out corresponding analyses for each night that included a clearly defined isoprene decline after dark (Supporting Information). Across those cases, we see significant variability in the importance of NO_3 chemistry, with mean isoprene lifetimes due to NO_3 ranging from 4 to >100 h. In most (10 of 13) cases, the resulting prediction for MVK + MACR agrees with the observations, thus corroborating the overall analysis. Occasionally, the agreement is not as good, for instance when MVK + MACR increased while isoprene was decreasing. These likely reflect situations when horizontal and/or vertical transport affected isoprene and its oxidation products differently. The nocturnal boundary layer (NBL) can be stratified with significant vertical gradients;^{20,46} such episodes could arise, for example, from downmixing of more photochemically aged air from aloft.

The SLAQRS observations thus point to the importance of NO_3 chemistry in removing isoprene overnight in this environment and to substantial variability in the efficacy of this process. We further confirmed the tenability of the above interpretation using the DSMACC chemical box model²⁸ (see the Methods for details). Figure S1 of the Supporting Information shows that, for the case with 0.5 ppb of NO , isoprene is efficiently oxidized by NO_3 and is largely removed overnight. Conversely, when NO_3 chemistry is suppressed by high NO , most isoprene (>5 ppb) is still present at dawn and available to undergo photochemical oxidation by OH.

Having large amounts of isoprene present at daybreak then provides a potent fuel to drive photochemistry the coming day. Figure 4 shows that days with high isoprene (>2 ppb) at 6 am and southerly winds had elevated morning ozone, averaging up to 26 ppb above the campaign mean (examples of individual days are shown in Figure 5). Furthermore, ozone on these days exhibited a dramatic morning peak that stands in stark contrast to the textbook scenario wherein ozone is highest during

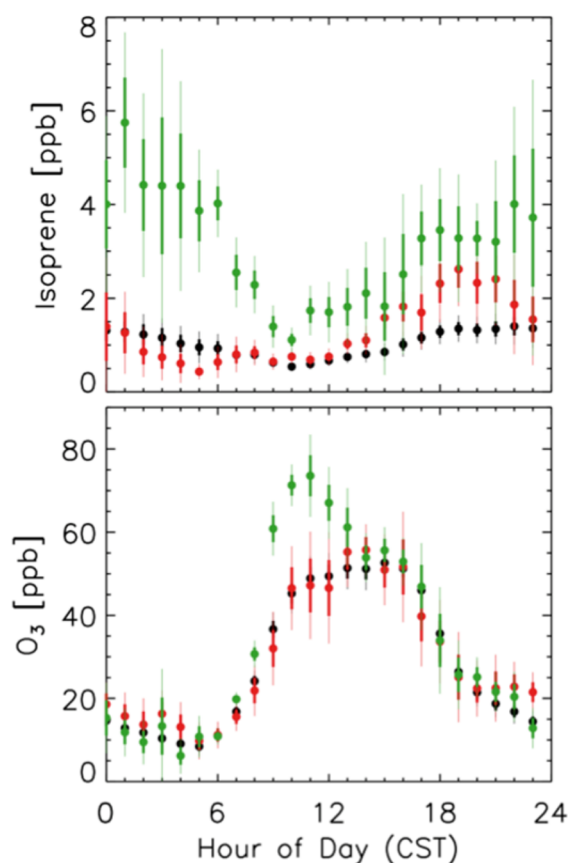


Figure 4. Diurnal cycle in isoprene and O_3 during summer in St. Louis. Mean observed concentrations by hour for the entire campaign (black) and for periods with southwesterly winds (170° – 270°) on days with (green, >2 ppb at 06:00) and without (red) elevated morning isoprene. Error bars show 1 (thick) and 2 (thin) standard deviations about the mean. Examples of individual days are shown in Figure 5. The corresponding O_x ($\text{O}_3 + \text{NO}_2$) plot is shown in the Supporting Information.

afternoon. Different averaging strategies modify somewhat the shape of this mean diurnal profile but not its overall attributes (see the Supporting Information). Thus, we see that the nighttime oxidation (or persistence) of isoprene has a powerful

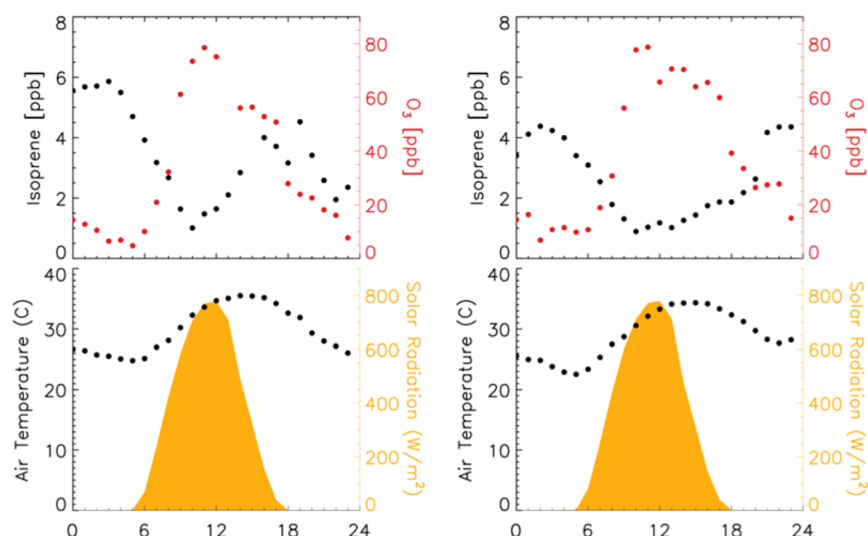


Figure 5. Examples of individual days with high morning isoprene (left, Sept 10, 2013; right, Sept 11, 2013).

bearing on ozone production and urban air quality the following day. The fact that isoprene at daybreak changes the daily timing of high ozone episodes also has ramifications for human health, for instance, affecting the scheduling of outdoor activities to minimize exposure.

Also shown in Figure 4 is the mean diurnal ozone profile for days with southwest winds that did not have high morning ozone. We see that mean ozone on these days does not differ significantly from the overall campaign mean. Days with high isoprene have higher than average temperatures (Supporting Information), as expected, because isoprene emissions depend exponentially upon temperature. Ozone production generally increases with temperature⁴⁷ due to, for example, accelerated chemistry, but this effect cannot explain the anomalous ozone diurnal profile that is observed. Entrainment from the overlying residual layer can also affect surface ozone. However, we should expect that injecting multiple parts per billion of isoprene into a high- NO_x urban environment at sunrise will drive substantial ozone production, and the DSMACC simulations support this. Figure S1 of the Supporting Information shows that the high- NO scenario with suppressed NO_3 chemistry does have substantially higher O_x ($\text{O}_3 + \text{NO}_2$) the following day compared to the base case with active NO_3 nighttime chemistry. However, this comparison is complicated by differing NO_x/VOC regimes in the two cases. We can better isolate the effect of isoprene itself and its overnight removal using a sensitivity simulation initialized in the same way as the base case but with all $\text{VOC} + \text{NO}_3$ reactions turned off. The results are shown in green in Figure S1 of the Supporting Information and predict a 10 ppb ozone enhancement when isoprene is present at daybreak relative to the base case in which most isoprene was oxidized by NO_3 the prior night. Critically, the predicted ozone enhancement peaks in the late morning, exactly as seen in the observations.

The magnitude of this ozone enhancement depends upon the uncertain fate of the organic nitrates produced by the isoprene + NO_3 reaction²¹ and the propensity of those remaining gas-phase nitrates to undergo photochemical oxidation the next day, potentially recycling NO_x versus deposition or aerosol uptake. We demonstrate this sensitivity in Figure S1 of the Supporting Information using a sensitivity simulation in which isoprene + NO_3 is assumed to represent a

terminal sink (i.e., the products are lost to surfaces or aerosol uptake, with no subsequent gas-phase chemistry or NO_x recycling). Using this as a baseline, we find that the ozone enhancement when isoprene is not removed overnight is nearly double (19 ppb) what it was using the standard model chemistry. Again, the ozone enhancement peaks in the late morning, as seen in the data.

4. IMPLICATIONS

We showed here that in an urban area downwind of an isoprene-emitting forest, peak isoprene concentrations of up to 8 ppb occur at night, despite isoprene's light-dependent source and short atmospheric lifetime. When significant isoprene is still present at dawn, it accelerates daytime photochemistry and changes its diurnal cycle, leading to a striking morning ozone peak that, in the mean, far exceeds values seen on other days (by as much as 26 ppb). This early onset also expands the daily window with persistently high ozone. Such events thus have important ramifications for meeting the U.S. ozone standard, which is defined on the basis of 8 h average concentrations. In fact, of the 4 days during this study with the highest 8 h O_3 values, two had high morning isoprene (on the basis of the criteria used earlier). These morning isoprene episodes could therefore determine whether or not cities such as St. Louis are in attainment with the federal ozone standard.

The amount of isoprene still present at daybreak, in turn, is strongly affected by its nighttime reaction with NO_3 . This biogenic–anthropogenic linkage involving nighttime isoprene and daytime ozone is likely to exhibit the opposite O_3 – NO_x dependence as would otherwise be expected within cities. For instance, as NO emissions decrease,⁴⁸ the degree of O_3 and NO_3 titration should diminish, leading to a more active role for NO_3 chemistry within the near-surface urban environment. For St. Louis and similar cities, this corresponds to more efficient nighttime isoprene removal and, hence, fewer daytime ozone enhancements. In parallel, aerosol mass could increase as a result of enhanced production of low-volatility isoprene (and terpene) nitrates.^{21,49–51} Outside of the urban core, NO_x reductions would likely reduce the importance of NO_3 chemistry (because of reduced formation via $\text{NO}_2 + \text{O}_3$), so that more isoprene survives the night to drive photochemistry and ozone production the following morning. Solely on the

basis of daytime chemistry, one would normally predict precisely the reverse tendency: NO_x reductions increasing ozone in the urban core while decreasing it in most other locations.

The above dynamics may vary in a complex way with altitude. The analyses here are based on surface measurements, and the chemical self-consistency from night to night and clear link to next day ozone both argue that our findings are spatially representative for the area and not merely controlled by local plumes. However, NO₃ chemistry can vary with height in the nighttime urban atmosphere²⁰ and may reach maximum efficiency at the interface between the NBL and overlying residual layer.⁵² Vertically resolved measurements probing the depth of the NBL and overlying residual layer are needed in this type of environment to more fully quantify the nighttime/daytime interactions explored here and to better understand how they are liable to change in the future.

■ ASSOCIATED CONTENT

■ Supporting Information

The Supporting Information is available free of charge on the ACS Publications website at DOI: 10.1021/acs.est.5b06367.

Figures S1–S6, discussion of potential measurement interferences, and attribution of nighttime trends in isoprene and MVK + MACR (PDF)

■ AUTHOR INFORMATION

Corresponding Author

*Telephone/Fax: 612-626-3259. E-mail: dbm@umn.edu.

Present Addresses

[‡]Munkhbayar Baasandorj: Utah Department of Environmental Quality, Salt Lake City, Utah 84116, United States.

[§]Lu Hu: Harvard University, Cambridge, Massachusetts 02138, United States.

Notes

The authors declare no competing financial interest.

■ ACKNOWLEDGMENTS

This work was supported by the National Science Foundation (Grant 1148951 to Dylan B. Millet), the United States Environmental Protection Agency (Grant R835402 to Brent J. Williams), and the Minnesota Supercomputing Institute.

■ REFERENCES

- (1) European Commission: Joint Research Centre JRC/Netherlands Environmental Assessment Agency PBL; *Emissions Database for Global Atmospheric Research (EDGAR)*, Version 4.2, 2011; <http://edgar.jrc.ec.europa.eu>.
- (2) Guenther, A. B.; Jiang, X.; Heald, C. L.; Sakulyanontvittaya, T.; Duhl, T.; Emmons, L. K.; Wang, X. The Model of Emissions of Gases and Aerosols from Nature version 2.1 (MEGAN2.1): an extended and updated framework for modeling biogenic emissions. *Geosci. Model Dev.* **2012**, *5* (6), 1471–1492.
- (3) Atkinson, R.; Baulch, D. L.; Cox, R. A.; Crowley, J. N.; Hampson, R. F.; Hynes, R. G.; Jenkin, M. E.; Rossi, M. J.; Troe, J.; IUPAC Subcommittee. Evaluated kinetic and photochemical data for atmospheric chemistry: Volume II - gas phase reactions of organic species. *Atmos. Chem. Phys.* **2006**, *6* (11), 3625–4055.
- (4) Sillman, S.; Logan, J. A.; Wofsy, S. C. The sensitivity of ozone to nitrogen oxides and hydrocarbons in regional ozone episodes. *J. Geophys. Res.* **1990**, *95*, 1837–1851.
- (5) Jaeglé, L.; Steinberger, L.; Martin, R. V.; Chance, K. Global partitioning of NO_x sources using satellite observations: Relative roles of fossil fuel combustion, biomass burning and soil emissions. *Faraday Discuss.* **2005**, *130*, 407–423.
- (6) Schumann, U.; Huntrieser, H. The global lightning-induced nitrogen oxides source. *Atmos. Chem. Phys.* **2007**, *7* (14), 3823–3907.
- (7) Trainer, M.; Williams, E. J.; Parrish, D. D.; Buhr, M. P.; Allwine, E. J.; Westberg, H. H.; Fehsenfeld, F. C.; Liu, S. C. Models and observations of the impact of natural hydrocarbons on rural ozone. *Nature* **1987**, *329* (6141), 705–707.
- (8) Chameides, W. L.; Lindsay, R. W.; Richardson, J.; Kiang, C. S. The role of biogenic hydrocarbons in urban photochemical smog: Atlanta as a case study. *Science* **1988**, *241* (4872), 1473–1475.
- (9) Kiendler-Scharr, A.; Wildt, J.; Dal Maso, M.; Hohaus, T.; Kleist, E.; Mentel, T. F.; Tillmann, R.; Uerlings, R.; Schurr, U.; Wahner, A. New particle formation in forests inhibited by isoprene emissions. *Nature* **2009**, *461* (7262), 381–384.
- (10) Carlton, A. G.; Pinder, R. W.; Bhawe, P. V.; Pouliot, G. A. To what extent can biogenic SOA be controlled? *Environ. Sci. Technol.* **2010**, *44* (9), 3376–3380.
- (11) Hoyle, C. R.; Boy, M.; Donahue, N. M.; Fry, J. L.; Glasius, M.; Guenther, A.; Hallar, A. G.; Hartz, K. H.; Petters, M. D.; Petaja, T.; Rosenoern, T.; Sullivan, A. P. A review of the anthropogenic influence on biogenic secondary organic aerosol. *Atmos. Chem. Phys.* **2011**, *11* (1), 321–343.
- (12) Xu, L.; Guo, H. Y.; Boyd, C. M.; Klein, M.; Bougiatioti, A.; Cerully, K. M.; Hite, J. R.; Isaacman-VanWertz, G.; Kreisberg, N. M.; Knote, C.; Olson, K.; Koss, A.; Goldstein, A. H.; Hering, S. V.; de Gouw, J.; Baumann, K.; Lee, S. H.; Nenes, A.; Weber, R. J.; Ng, N. L. Effects of anthropogenic emissions on aerosol formation from isoprene and monoterpenes in the southeastern United States. *Proc. Natl. Acad. Sci. U. S. A.* **2015**, *112* (1), 37–42.
- (13) Horowitz, L. W.; Fiore, A. M.; Milly, G. P.; Cohen, R. C.; Perring, A.; Wooldridge, P. J.; Hess, P. G.; Emmons, L. K.; Lamarque, J. F. Observational constraints on the chemistry of isoprene nitrates over the eastern United States. *J. Geophys. Res.* **2007**, *112* (D12), D12S08.
- (14) Perring, A. E.; Bertram, T. H.; Wooldridge, P. J.; Fried, A.; Heikes, B. G.; Dibb, J.; Crounse, J. D.; Wennberg, P. O.; Blake, N. J.; Blake, D. R.; Brune, W. H.; Singh, H. B.; Cohen, R. C. Airborne observations of total RONO₂: new constraints on the yield and lifetime of isoprene nitrates. *Atmos. Chem. Phys.* **2009**, *9* (4), 1451–1463.
- (15) Mao, J.; Paulot, F.; Jacob, D. J.; Cohen, R. C.; Crounse, J. D.; Wennberg, P. O.; Keller, C. A.; Hudman, R. C.; Barkley, M. P.; Horowitz, L. W. Ozone and organic nitrates over the eastern United States: Sensitivity to isoprene chemistry. *J. Geophys. Res. Atmos.* **2013**, *118*, 11256–11268.
- (16) Sharkey, T. D.; Yeh, S. S. Isoprene emission from plants. *Annu. Rev. Plant Physiol. Plant Mol. Biol.* **2001**, *52*, 407–436.
- (17) Pressley, S.; Lamb, B.; Westberg, H.; Flaherty, J.; Chen, J.; Vogel, C. Long-term isoprene flux measurements above a northern hardwood forest. *J. Geophys. Res.* **2005**, *110* (D7), D07301.
- (18) Stroud, C. A.; Roberts, J. M.; Williams, E. J.; Hereid, D.; Angevine, W. M.; Fehsenfeld, F. C.; Wisthaler, A.; Hansel, A.; Martinez-Harder, M.; Harder, H.; Brune, W. H.; Hoenninger, G.; Stutz, J.; White, A. B. Nighttime isoprene trends at an urban forested site during the 1999 Southern Oxidant Study. *J. Geophys. Res.* **2002**, *107* (D16), 4291.
- (19) Brown, S. S.; Degouw, J. A.; Warneke, C.; Ryerson, T. B.; Dube, W. P.; Atlas, E.; Weber, R. J.; Peltier, R. E.; Neuman, J. A.; Roberts, J. M.; Swanson, A.; Flocke, F.; McKeen, S. A.; Brioude, J.; Sommariva, R.; Trainer, M.; Fehsenfeld, F. C.; Ravishankara, A. R. Nocturnal isoprene oxidation over the Northeast United States in summer and its impact on reactive nitrogen partitioning and secondary organic aerosol. *Atmos. Chem. Phys.* **2009**, *9* (9), 3027–3042.
- (20) Brown, S. S.; Stutz, J. Nighttime radical observations and chemistry. *Chem. Soc. Rev.* **2012**, *41* (19), 6405–6447.
- (21) Rollins, A. W.; Kiendler-Scharr, A.; Fry, J. L.; Brauers, T.; Brown, S. S.; Dorn, H. P.; Dube, W. P.; Fuchs, H.; Mensah, A.; Mentel, T. F.; Rohrer, F.; Tillmann, R.; Wegener, R.; Wooldridge, P. J.; Cohen,

- R. C. Isoprene oxidation by nitrate radical: alkyl nitrate and secondary organic aerosol yields. *Atmos. Chem. Phys.* **2009**, *9* (18), 6685–6703.
- (22) Starn, T. K.; Shepson, P. B.; Bertman, S. B.; Riemer, D. D.; Zika, R. G.; Olszyna, K. Nighttime isoprene chemistry at an urban-impacted forest site. *J. Geophys. Res.* **1998**, *103* (D17), 22437–22447.
- (23) Lee, J. H.; Hopke, P. K.; Turner, J. R. Source identification of airborne PM_{2.5} at the St. Louis-Midwest Supersite. *J. Geophys. Res.* **2006**, *111* (D10), D10S10.
- (24) Wang, G. L.; Hopke, P. K.; Turner, J. R. Using highly time resolved fine particulate compositions to find particle sources in St. Louis, MO. *Atmos. Pollut. Res.* **2011**, *2* (2), 219–230.
- (25) Hu, L.; Millet, D. B.; Mohr, M. J.; Wells, K. C.; Griffis, T. J.; Helmig, D. Sources and seasonality of atmospheric methanol based on tall tower measurements in the US Upper Midwest. *Atmos. Chem. Phys.* **2011**, *11* (21), 11145–11156.
- (26) Hu, L.; Millet, D. B.; Kim, S. Y.; Wells, K. C.; Griffis, T. J.; Fischer, E. V.; Helmig, D.; Hueber, J.; Curtis, A. J. North American acetone sources determined from tall tower measurements and inverse modeling. *Atmos. Chem. Phys.* **2013**, *13* (6), 3379–3392.
- (27) Baasandorj, M.; Millet, D. B.; Hu, L.; Mitroo, D.; Williams, B. J. Measuring acetic and formic acid by proton-transfer-reaction mass spectrometry: sensitivity, humidity dependence, and quantifying interferences. *Atmos. Meas. Tech.* **2015**, *8*, 1303–1321.
- (28) Emmerson, K. M.; Evans, M. J. Comparison of tropospheric gas-phase chemistry schemes for use within global models. *Atmos. Chem. Phys.* **2009**, *9* (5), 1831–1845.
- (29) Andres-Hernandez, M. D.; Stone, D.; Brookes, D. M.; Commane, R.; Reeves, C. E.; Huntrieser, H.; Heard, D. E.; Monks, P. S.; Burrows, J. P.; Schlager, H.; Kartal, D.; Evans, M. J.; Floquet, C. F. A.; Ingham, T.; Methven, J.; Parker, A. E. Peroxy radical partitioning during the AMMA radical intercomparison exercise. *Atmos. Chem. Phys.* **2010**, *10* (21), 10621–10638.
- (30) Millet, D. B.; Guenther, A.; Siegel, D. A.; Nelson, N. B.; Singh, H. B.; de Gouw, J. A.; Warneke, C.; Williams, J.; Eerdekens, G.; Sinha, V.; Karl, T.; Flocke, F.; Apel, E.; Riemer, D. D.; Palmer, P. I.; Barkley, M. Global atmospheric budget of acetaldehyde: 3D model analysis and constraints from in-situ and satellite observations. *Atmos. Chem. Phys.* **2010**, *10*, 3405–3425.
- (31) Stone, D.; Evans, M. J.; Commane, R.; Ingham, T.; Floquet, C. F. A.; McQuaid, J. B.; Brookes, D. M.; Monks, P. S.; Purvis, R.; Hamilton, J. F.; Hopkins, J.; Lee, J.; Lewis, A. C.; Stewart, D.; Murphy, J. G.; Mills, G.; Oram, D.; Reeves, C. E.; Heard, D. E. HO_x observations over West Africa during AMMA: impact of isoprene and NO_x. *Atmos. Chem. Phys.* **2010**, *10* (19), 9415–9429.
- (32) Sandu, A.; Sander, R. Technical note: Simulating chemical systems in Fortran90 and Matlab with the Kinetic PreProcessor KPP-2.1. *Atmos. Chem. Phys.* **2006**, *6*, 187–195.
- (33) National Center for Atmospheric Research NCAR/ACOM; Tropospheric Ultraviolet and Visible (TUV) Radiation Model; <https://www2.acom.ucar.edu/modeling/tropospheric-ultraviolet-and-visible-tuv-radiation-model>.
- (34) Wiedinmyer, C.; Greenberg, J.; Guenther, A.; Hopkins, B.; Baker, K.; Geron, C.; Palmer, P. I.; Long, B. P.; Turner, J. R.; Petron, G.; Harley, P.; Pierce, T. E.; Lamb, B.; Westberg, H.; Baugh, W.; Koerber, M.; Janssen, M. Ozarks Isoprene Experiment (OZIE): Measurements and modeling of the “isoprene volcano”. *J. Geophys. Res.* **2005**, *110* (D18), D18307.
- (35) Potosnak, M. J.; LeStourgeon, L.; Pallardy, S. G.; Hosman, K. P.; Gu, L. H.; Karl, T.; Geron, C.; Guenther, A. B. Observed and modeled ecosystem isoprene fluxes from an oak-dominated temperate forest and the influence of drought stress. *Atmos. Environ.* **2014**, *84*, 314–322.
- (36) Seco, R.; Karl, T.; Guenther, A.; Hosman, K. P.; Pallardy, S. G.; Gu, L. H.; Geron, C.; Harley, P.; Kim, S. Ecosystem-scale volatile organic compound fluxes during an extreme drought in a broadleaf temperate forest of the Missouri Ozarks (central USA). *Glob. Change Biol.* **2015**, *21* (10), 3657–3674.
- (37) Millet, D. B.; Baasandorj, M.; Farmer, D. K.; Thornton, J. A.; Baumann, K.; Brophy, P.; Chaliyakunnel, S.; de Gouw, J. A.; Graus, M.; Hu, L.; Koss, A.; Lee, B. H.; Lopez-Hilfiker, F. D.; Neuman, J. A.; Paulot, F.; Peischl, J.; Pollack, I. B.; Ryerson, T. B.; Warneke, C.; Williams, B. J.; Xu, J. A large and ubiquitous source of atmospheric formic acid. *Atmos. Chem. Phys.* **2015**, *15* (11), 6283–6304.
- (38) Apel, E. C.; Riemer, D. D.; Hills, A.; Baugh, W.; Orlando, J.; Faloon, I.; Tan, D.; Brune, W.; Lamb, B.; Westberg, H.; Carroll, M. A.; Thornberry, T.; Geron, C. D. Measurement and interpretation of isoprene fluxes and isoprene, methacrolein, and methyl vinyl ketone mixing ratios at the PROPHET site during the 1998 Intensive. *J. Geophys. Res.* **2002**, *107* (D3), 4034.
- (39) Kaiser, J.; Skog, K. M.; Baumann, K.; Bertman, S. B.; Brown, S. B.; Brune, W. H.; Crounse, J. D.; de Gouw, J. A.; Edgerton, E. S.; Feiner, P. A.; Goldstein, A. H.; Koss, A.; Misztal, P. K.; Nguyen, T. B.; Olson, K. F.; St. Clair, J. M.; Teng, A. P.; Toma, S.; Wennberg, P. O.; Wild, R. J.; Zhang, L.; Keutsch, F. N. Speciation of OH reactivity above the canopy of an isoprene-dominated forest. *Atmos. Chem. Phys. Discuss.* **2016**, *1* DOI: 10.5194/acp-2015-1006.
- (40) Aschmann, S. M.; Atkinson, R. Formation yields of methyl vinyl ketone and methacrolein from the gas-phase reaction of O₃ with isoprene. *Environ. Sci. Technol.* **1994**, *28* (8), 1539–1542.
- (41) Kwok, E. S. C.; Aschmann, S. M.; Arey, J.; Atkinson, R. Product formation from the reaction of the NO₃ radical with isoprene and rate constants for the reactions of methacrolein and methyl vinyl ketone with the NO₃ radical. *Int. J. Chem. Kinet.* **1996**, *28* (12), 925–934.
- (42) Paulot, F.; Crounse, J. D.; Kjaergaard, H. G.; Kroll, J. H.; Seinfeld, J. H.; Wennberg, P. O. Isoprene photooxidation: new insights into the production of acids and organic nitrates. *Atmos. Chem. Phys.* **2009**, *9* (4), 1479–1501.
- (43) de Gouw, J. A.; Middlebrook, A. M.; Warneke, C.; Goldan, P. D.; Kuster, W. C.; Roberts, J. M.; Fehsenfeld, F. C.; Worsnop, D. R.; Canagaratna, M. R.; Pszenny, A. A. P.; Keene, W. C.; Marchewka, M.; Bertman, S. B.; Bates, T. S. Budget of organic carbon in a polluted atmosphere: Results from the New England Air Quality Study in 2002. *J. Geophys. Res.* **2005**, *110* (D16), D16305.
- (44) Hu, L.; Millet, D. B.; Baasandorj, M.; Griffis, T. J.; Turner, P.; Helmig, D.; Curtis, A. J.; Hueber, J. Isoprene emissions and impacts over an ecological transition region in the US Upper Midwest inferred from tall tower measurements. *J. Geophys. Res.* **2015**, *120*, 3553–3571.
- (45) Wolfe, G. M.; Kaiser, J.; Hanisco, T. F.; Keutsch, F. N.; de Gouw, J. A.; Gilman, J. B.; Graus, M.; Hatch, C. D.; Holloway, J.; Horowitz, L. W.; Lee, B. H.; Lerner, B. M.; Lopez-Hilfiker, F.; Mao, J.; Marvin, M. R.; Peischl, J.; Pollack, I. B.; Roberts, J. M.; Ryerson, T. B.; Thornton, J. A.; Veres, P. R.; Warneke, C. Formaldehyde production from isoprene oxidation across NO_x regimes. *Atmos. Chem. Phys.* **2016**, *16*, 2597–2610.
- (46) Stutz, J.; Wong, K. W.; Lawrence, L.; Ziemba, L.; Flynn, J. H.; Rappengluck, B.; Lefer, B. Nocturnal NO₃ radical chemistry in Houston, TX. *Atmos. Environ.* **2010**, *44* (33), 4099–4106.
- (47) Lin, C.-Y. C.; Jacob, D. J.; Fiore, A. M. Trends in exceedances of the ozone air quality standard in the continental United States, 1980–1998. *Atmos. Environ.* **2001**, *35* (19), 3217–3228.
- (48) Russell, A. R.; Valin, L. C.; Cohen, R. C. Trends in OMI NO₂ observations over the United States: effects of emission control technology and the economic recession. *Atmos. Chem. Phys.* **2012**, *12* (24), 12197–12209.
- (49) Ng, N. L.; Kwan, A. J.; Surratt, J. D.; Chan, A. W. H.; Chhabra, P. S.; Sorooshian, A.; Pye, H. O. T.; Crounse, J. D.; Wennberg, P. O.; Flagan, R. C.; Seinfeld, J. H. Secondary organic aerosol (SOA) formation from reaction of isoprene with nitrate radicals (NO₃). *Atmos. Chem. Phys.* **2008**, *8* (14), 4117–4140.
- (50) Rollins, A. W.; Browne, E. C.; Min, K. E.; Pusede, S. E.; Wooldridge, P. J.; Gentner, D. R.; Goldstein, A. H.; Liu, S.; Day, D. A.; Russell, L. M.; Cohen, R. C. Evidence for NO_x control over nighttime SOA formation. *Science* **2012**, *337* (6099), 1210–1212.
- (51) Fry, J. L.; Draper, D. C.; Barsanti, K. C.; Smith, J. N.; Ortega, J.; Winkler, P. M.; Lawler, M. J.; Brown, S. S.; Edwards, P. M.; Cohen, R. C.; Lee, L. Secondary organic aerosol formation and organic nitrate yield from NO₃ oxidation of biogenic hydrocarbons. *Environ. Sci. Technol.* **2014**, *48* (20), 11944–11953.

(52) Geyer, A.; Stutz, J. The vertical structure of OH-HO₂-RO₂ chemistry in the nocturnal boundary layer: A one-dimensional model study. *J. Geophys. Res.* **2004**, *109* (D16), D16301.